Topographic data analysis for the VERITAS 2023 Iceland field campaign

G. Cascioli[1,2], B. Carr[3], E. Mazarico[2], D. Nunes[4], C.W. Hamilton[3], J.C. Andrews-Hanna[3], O.C. Knox[3], M.C. Raguso4, J. Whitten[5], D. Buczkowski[6], S. Smrekar[4] & The VERITAS 2023 Iceland Field Team

Introduction and motivation

The NASA Discovery mission VERITAS (Venus Emissivity, Radio Science, InSAR, Topography, and Spectroscopy) will explore Venus in the early 2030s, acquiring foundational global datasets that will reshape our understanding of planetary evolution. Its synthetic aperture radar (VISAR) will globally map the surface at X-band wavelength (~3 cm). To better interpret the radar backscatter measurements, relate them to physical properties such as surface roughness, and intercompare them with other radar datasets (Magellan S-band and EnVision VenSAR S-band), the VERITAS science team conducted a field campaign in Iceland, in collaboration with a multi-band radar mapping airborne campaign.
Using a combination of Terrestrial Laser Scanners (TLS) and Unmanned Aerial Systems (UAS) we collected topographic information at >40 sites, with the goal of characterizing a wide spectrum of terrains and geologic units.

The goal of the analysis of the topographic information of these terrains consists in understanding:
1) Effect of wavelength on the geometrical characteristics of the terrain (roughness, slope, relevant for radar)
2) Effect of posting and resolution on the apparent characteristics of the terrain
3) Information content of different geometric measures for clustering different terrains

Context pictures and topographic relief of three different locations representative diverse terrains investigated during the field campaign.

Left terrain consists in a fractured spiny basalt, located in the Holuhraun Hot Springs area.

Center terrain is representative of a pre-existing flow partially covered with sediments (tephra). This terrain is particularly interesting because of the significant diversity of characteristics over short length scales

Right terrain consists in a ropy basaltic flow with a characteristic (directional) repetitiveness.

Spiny basalt

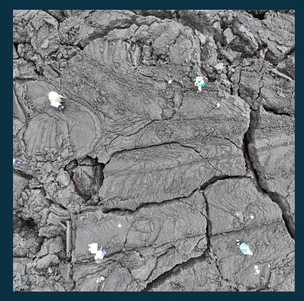

HLHS02P1

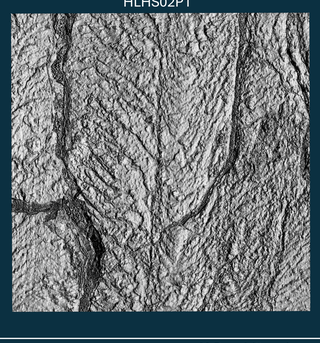

A'a flow partially covered with tephra

ASNF01P1

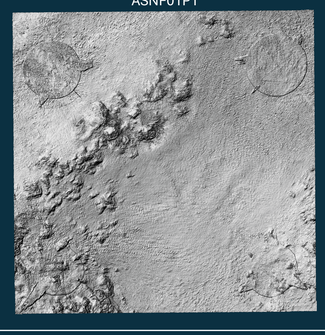

2021 Fagradalsfjall flow re-extruded from the overlying 2022 flow

FF2205P1

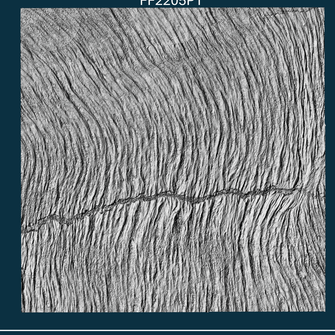

Attempts at automated clustering

Fine sampling of the investigated terrains enables their spectral characterization. This means that different characteristics (slope, roughness, elevation) can be studied at different characteristic sampling wavelengths.

As shown in another box (*Local fractal characteristics*) specific features will modify the spectrum from a simple power law (fractal), thus possibly identifying the terrain type.
We have attempted automated clustering of the 41 different terrain patches imaged during the field campaign. To assess the success of the automated clustering, we compare it to manual clustering results, based on visual inspection.

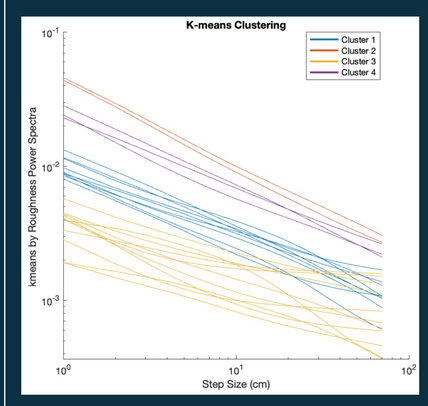

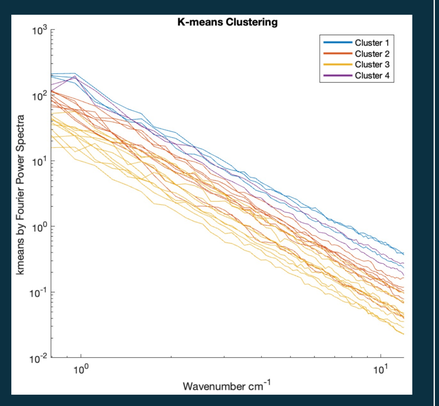

The automated classifier (k-means clustering) was run using either the power spectrum of the elevation or the roughness spectrum, as an observable. The results differ in the two cases, but generally align in finding the optimal number of classes as 4. The automated classification, differs from the manual classification. This is mainly due to the criterion adopted for manual classification, based on visual inspection.

Next developments will involve using multiple information sources for the classifier (roughness, elevation and slope) together with allowing the complexity to grow, by classifying sub-regions of single patches, instead of the patch as a whole.

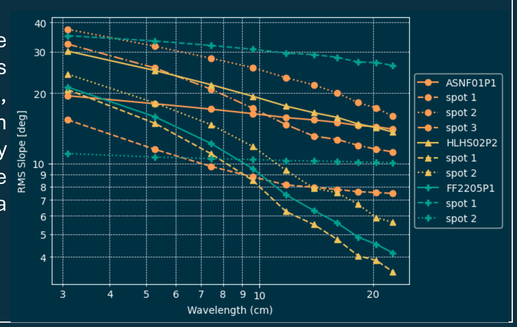

Effect of wavelength

Different wavelengths interact differently with the characteristic features of the terrain. To visually represent this effect, we computed the slope and roughness of these three terrains with sliding windows of different width. We show, for each terrain, the slope and roughness computed with window sizes equivalent to the S and X radio bands, representative of the Magellan (S-band) and VERITAS (X-band) SAR products.

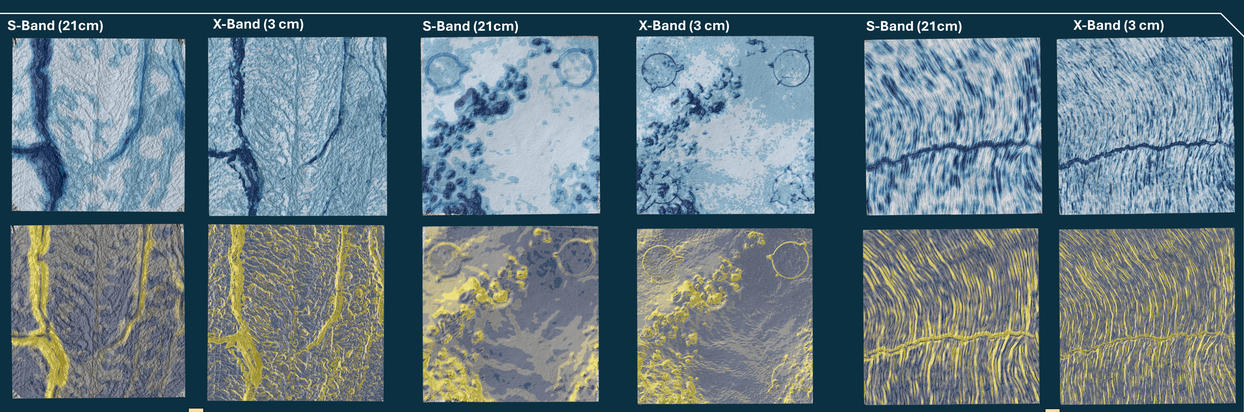

Effect of sampling and posting

As expected, coarser posting, leads to the same qualitative conclusions as compared to finer values (finer gridding).

The underlying DEM sampling resolution has a strong effect on the resulting values.

While maintaining the qualitative characteristics of the terrain, the quantitative results may strongly differ. For example, the rougher pixel (max RMS height) can move across the terrain, changing the interpretation of the scene.

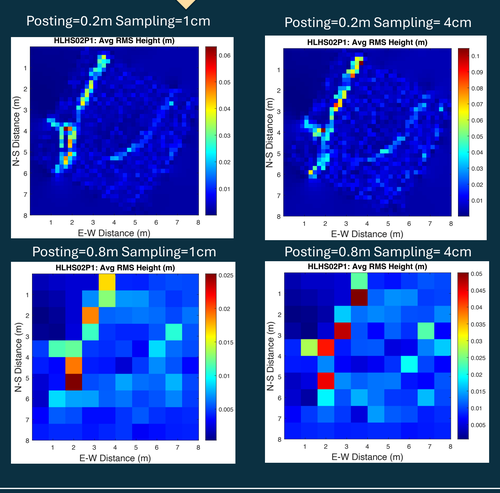

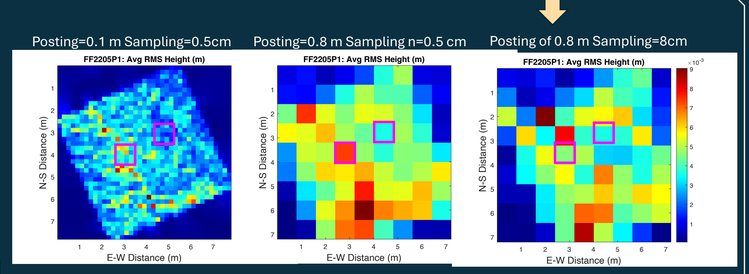

An example of the strong effect of sampling on the final product. At the same posting scale, different sampling leads to different values of the roughness.
Importantly, not only the absolute value of the roughness changes (which is expected) but also the relative values among pixels differs.
In the example above, when changing from 0.5 to 8cm sampling, the "high roughness" pixels move across the scene.

Local fractal characteristics

The ropy lava terrain is particularly interesting because it shows repetitive features, regions of high and low roughness. It is an interesting test case to understand how these characteristics map out at lower resolutions (lower posting) and how they impact the fractal characteristics (i.e., the spectrum)
The two highlighted pixels on the right show (average) high and low roughness regions, with different periodicities. The low roughness region has a periodic shape at around 10cm wavelength, while the high roughness region ~30cm. These periodicities are well captured by the power spectrum

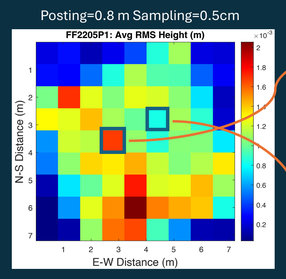

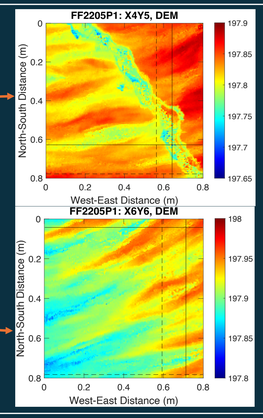

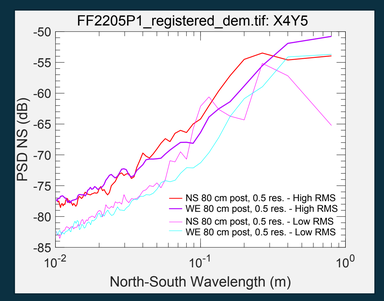

Explore the VERITAS science!

Smrekar & the VERITAS science team (#1763, Tomorrow 2.20 PM)
Nakaya et al . (#2583), Li et al. (#2617)
VISAR: Mendoza et al . (#1770)
VEM: Alemanno et al . (#1824), Garland et al . (#1029), Plesa et al . (#2079)
Gravity Science: Gülcher et al . (#1936), Baccarin et al . (#1903), Mazarico et al . (#1771)
Iceland 2023 Field Campaign: Hong et al . (#1844), Matsko et al . (#1549), Adeli et al . (#2484), Cascioli et al . (#1893), Whitten et al . (#2220), Nunes et al . (#1591), Hensley et al . (#1440), Raguso et al . (#2037)

Acknowledgements

GC and EM were funded by the NASA Planetary Science Division Research Program through the GSFC GIFT ISFM. A portion of this work was conducted at the Jet Propulsion Laboratory, California Institute of Technology, under contract with NASA.

(1) UMBC (2) NASA Goddard Space Flight Center (3) (4) NASA Jet Propulsion Laboratory California Institute of Technology (5) Smithsonian (6) APL